Supporting Information

2D low-buckled hexagonal honeycomb Weyl-point spin-gapless semiconductor family with quantum anomalous Hall effect

Weihua Zhang,[1] Jie Zhang,[1] Shoubing Ding,[1,*] Zhenxiang Cheng,[2,*] Zhimin Wu[1,*]

[1]*School of Physics and Electronic Engineering, Chongqing Normal University, Chongqing 401331, China*

[2]*Institute for Superconducting and Electronic Materials (ISEM), University of Wollongong, Wollongong 2500, Australia.*

[*]*Corresponding author: shoubingding@cqnu.edu.cn;*

cheng@uow.edu.au;

zmwu@cqnu.edu.cn

TABLE. S1. The Lattice constants *a*, bond lengths $l_{\text{Li-}Y}$ and $l_{\text{Li-}Y}$ and cohesive energies E_c of Li*XY* monolayers. $E_{\text{g-slab}}$ and $E_{\text{g-bulk}}$ are bandgaps of Li*XY* monolayers and bulk Li*XY*, respectively.

Systems	*A* (Å)	$l_{\text{Li-}Y}$ (Å)	$l_{X\text{-}Y}$ (Å)	E_c (eV/atom)	$E_{\text{g-slab}}$ (eV)	$E_{\text{g-bulk}}$ (eV)[1]
LiMgP	4.15	2.56	2.49	2.63	1.78	1.54
LiMgAs	4.29	2.64	2.58	2.44	1.57	1.37
LiZnP	4.00	2.53	2.34	2.36	1.61	1.35
LiZnAs	4.16	2.61	2.44	2.15	1.09	0.49
LiCdP	4.27	2.59	2.56	2.12	1.21	0.56
LiCdAs	4.42	2.66	2.66	1.96	0.81	0

1 S. Kacimi, H. Mehnane and A. Zaoui, J. Alloys Compd., 2014, 587, 451-458. https://doi.org/10.1016/j.jallcom.2013.10.046

TABLE. S2. The Energies of ferromagnetic configuration for $Li_{12}X_{10}Cr_2Y_{12}$ monolayers E_{FM} and the energy differences between ferromagnetic and antiferromagnetic configurations ΔE.

Systems	E_{FM} (eV)	$\Delta E_{(AFM-1)-FM}$ (meV)	$\Delta E_{(AFM-2)-FM}$ (meV)	$\Delta E_{(AFM-3)-FM}$ (meV)
$Li_{12}Mg_{10}Cr_2P_{12}$	-265.38	480.07	90.02	26.95
$Li_{12}Mg_{10}Cr_2As_{12}$	-246.74	457.48	88.82	26.47
$Li_{12}Zn_{10}Cr_2P_{12}$	-250.58	531.48	87.15	27.92
$Li_{12}Zn_{10}Cr_2As_{12}$	-230.52	451.67	82.37	25.83
$Li_{12}Cd_{10}Cr_2P_{12}$	-235.50	468.03	79.60	26.57
$Li_{12}Cd_{10}Cr_2As_{12}$	-218.83	391.43	72.12	23.24

TABLE. S3. Magnetic exchange coupling parameters J_2^{α} and J_3^{α}.

Systems	J_2^x (meV)	J_2^y (meV)	J_2^z (meV)	J_3^x (meV)	J_3^y (meV)	J_3^z (meV)
$Li_{12}Mg_{10}Cr_2P_{12}$	-0.23	-0.23	-0.23	-0.08	-0.08	-0.08
$Li_{12}Mg_{10}Cr_2As_{12}$	-0.19	-0.19	-0.20	-0.10	-0.10	-0.10
$Li_{12}Zn_{10}Cr_2P_{12}$	-0.32	-0.32	-0.32	-0.06	-0.06	-0.06
$Li_{12}Zn_{10}Cr_2As_{12}$	-0.21	-0.21	-0.22	-0.10	-0.10	-0.10
$Li_{12}Cd_{10}Cr_2P_{12}$	-0.24	-0.24	-0.23	-0.12	-0.12	-0.12
$Li_{12}Cd_{10}Cr_2As_{12}$	-0.17	-0.17	-0.17	-0.12	-0.12	-0.11

TABLE. S4. Atomic and total magnetic moments for $Li_{12}X_{10}Cr_2Y_{12}$ monolayers.

Systems	Li (μ_B)	*X* (μ_B)	Cr (μ_B)	*Y* (nearest of Cr / others) (μ_B)	Total (μ_B)
$Li_{12}Mg_{10}Cr_2P_{12}$	0	0.01	3.57	-0.05 / 0	6.91
$Li_{12}Mg_{10}Cr_2As_{12}$	0	0.01	3.67	-0.06 / 0	7.06
$Li_{12}Zn_{10}Cr_2P_{12}$	0	0.01	3.54	-0.05 / 0	6.94
$Li_{12}Zn_{10}Cr_2As_{12}$	0	0.01	3.64	-0.05 / 0	7.09
$Li_{12}Cd_{10}Cr_2P_{12}$	0	0.01	3.53	-0.06 / 0	6.94
$Li_{12}Cd_{10}Cr_2As_{12}$	0	0.01	3.63	-0.06 / 0	7.08

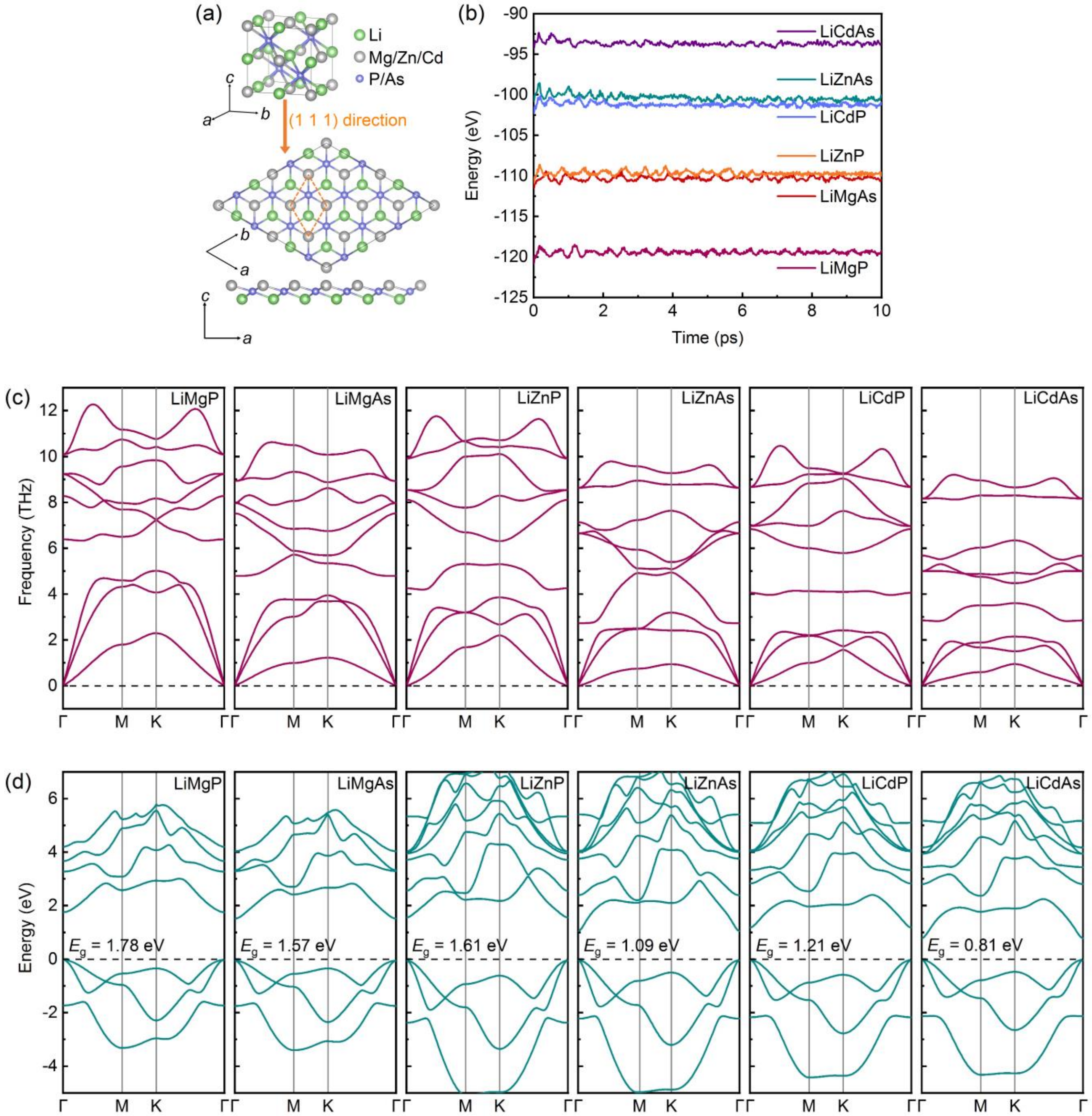

FIG. S1. (a) Top and side view of Li*XY* (*X* = Mg, Zn, Cd; *Y* = P, As) monolayers with lattice vectors *a*, *b* and *c*. (b) Total potential energy fluctuations of Li*XY* monolayers during AIMD simulations at 300 K. (c) Phonon spectra of Li*XY* monolayers. (d) Electronic band structures of Li*XY* monolayers.

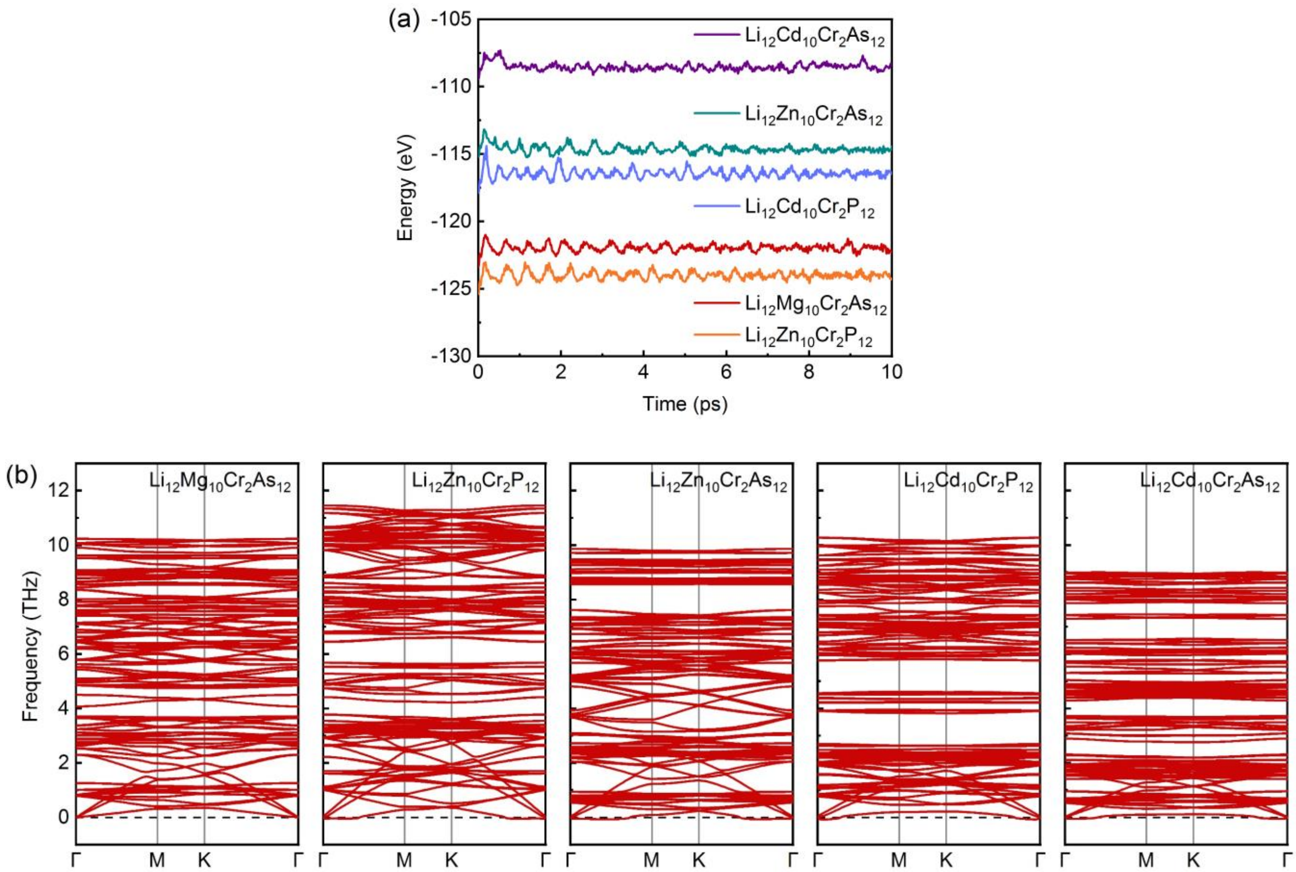

FIG. S2. (a) Total potential energy fluctuations of $Li_{12}X_{10}Cr_2Y_{12}$ (X = Mg, Zn, Cd; Y = P, As) monolayers during AIMD simulations at 300 K. (b) Phonon spectra of $Li_{12}X_{10}Cr_2Y_{12}$ monolayers.

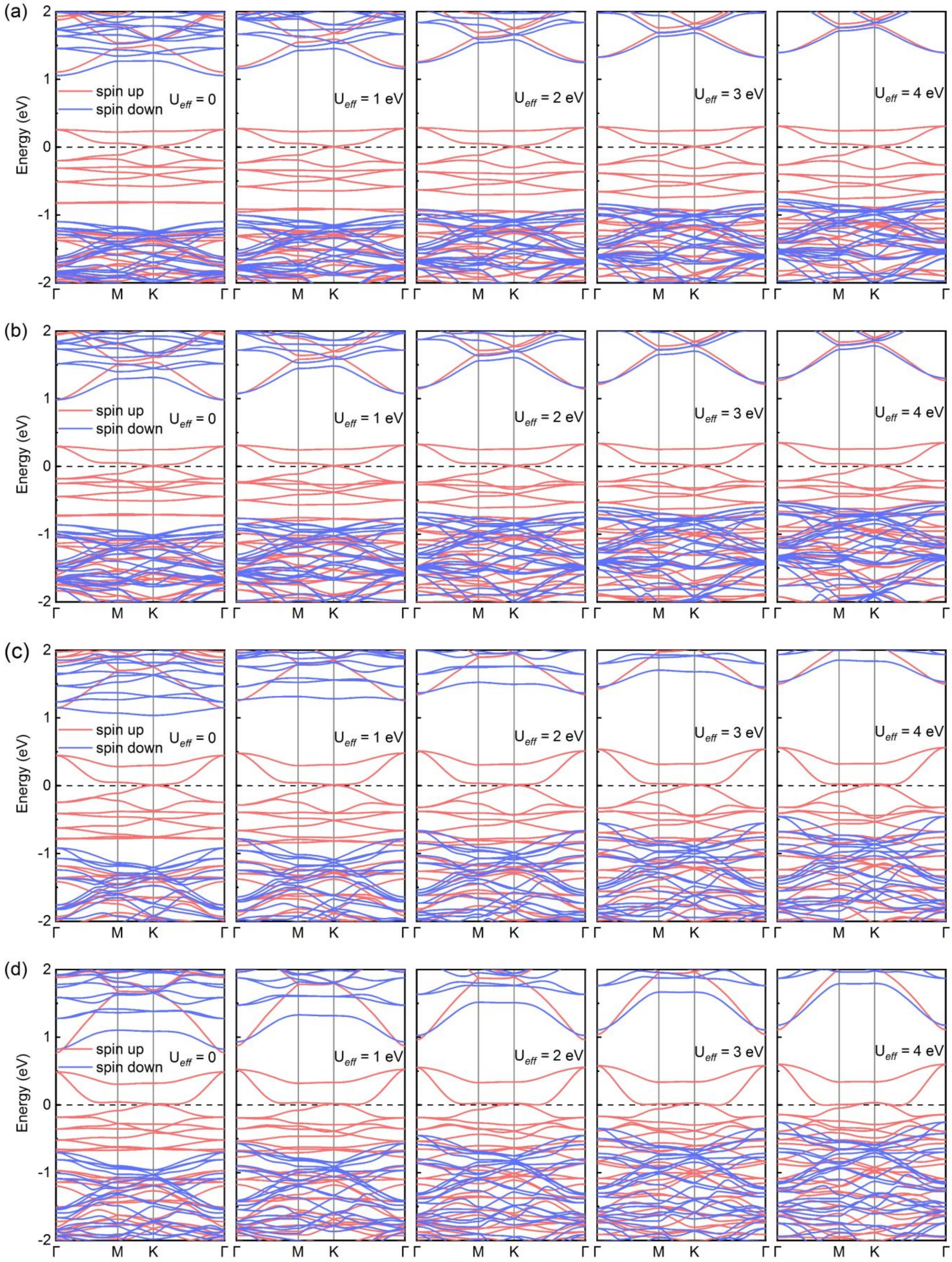
(a)
(b)
(c)
(d)
Energy (eV)
spin up
spin down
U_eff = 0
U_eff = 1 eV
U_eff = 2 eV
U_eff = 3 eV
U_eff = 4 eV
Γ
M
K
Γ

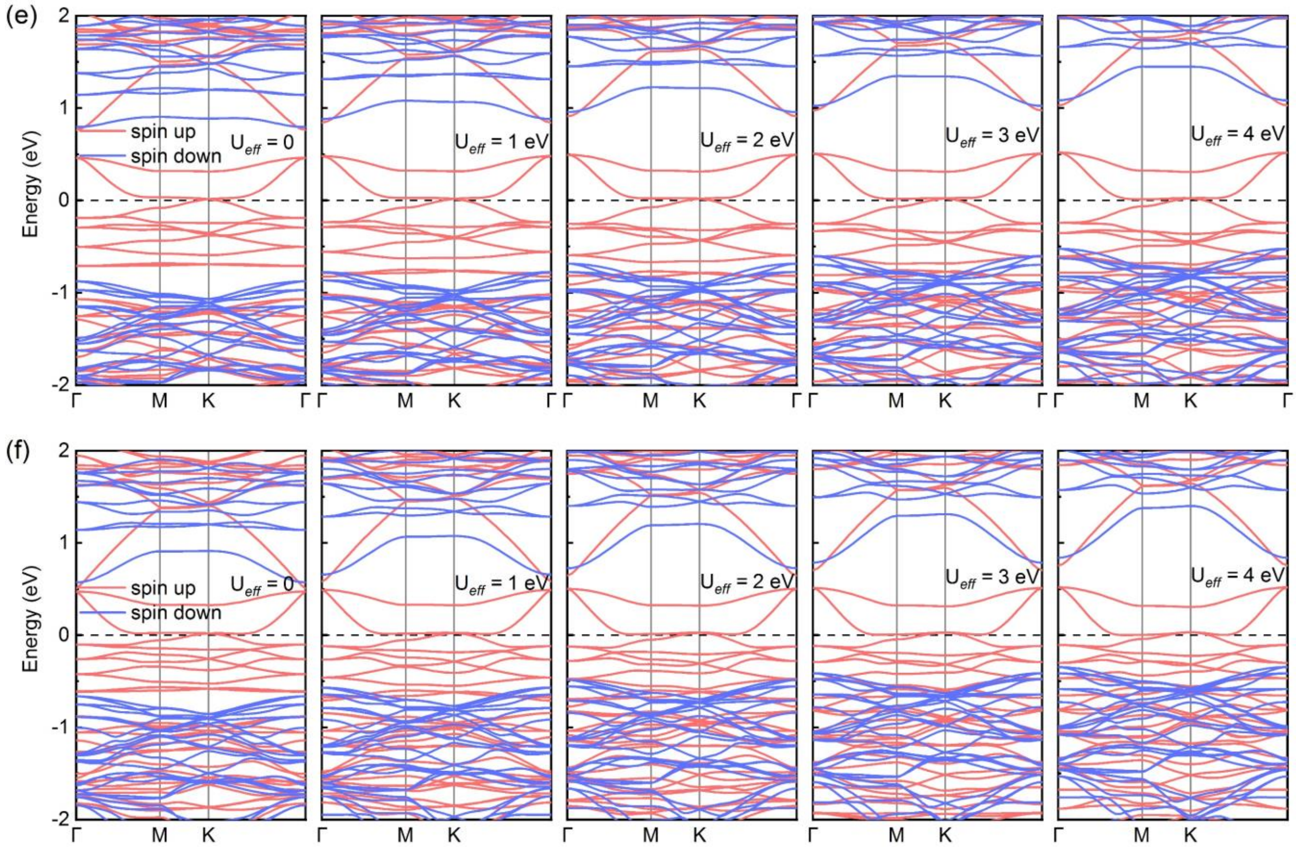

FIG. S3. Electronic band structures without SOC at different effective U (U_{eff}) values (U_{eff} = 1, 2, 3, 4 eV) of the Cr atom for (a) $Li_{12}Mg_{10}Cr_2P_{12}$ monolayer, (b) $Li_{12}Mg_{10}Cr_2As_{12}$ monolayer, (c) $Li_{12}Zn_{10}Cr_2P_{12}$ monolayer, (d) $Li_{12}Zn_{10}Cr_2As_{12}$ monolayer, (e) $Li_{12}Cd_{10}Cr_2P_{12}$ monolayer and (f) $Li_{12}Cd_{10}Cr_2As_{12}$ monolayer, respectively.

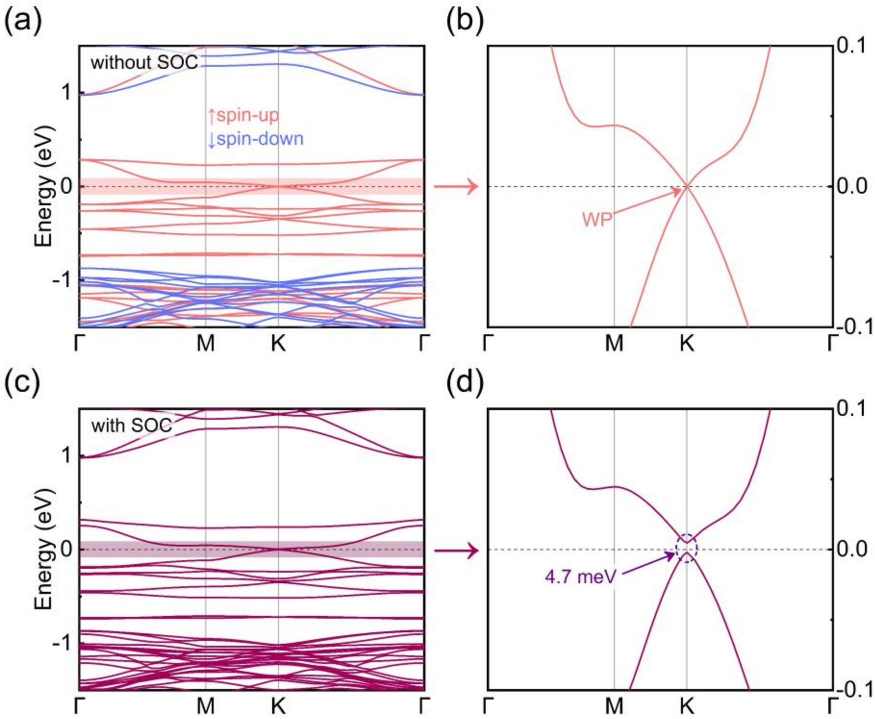

FIG. S4. Calculated electronic band structures of the $Li_{12}Mg_{10}Cr_2As_{12}$ monolayer (a) without SOC and (c) with SOC. (b) and (d) are enlarged view around the Fermi energy level.

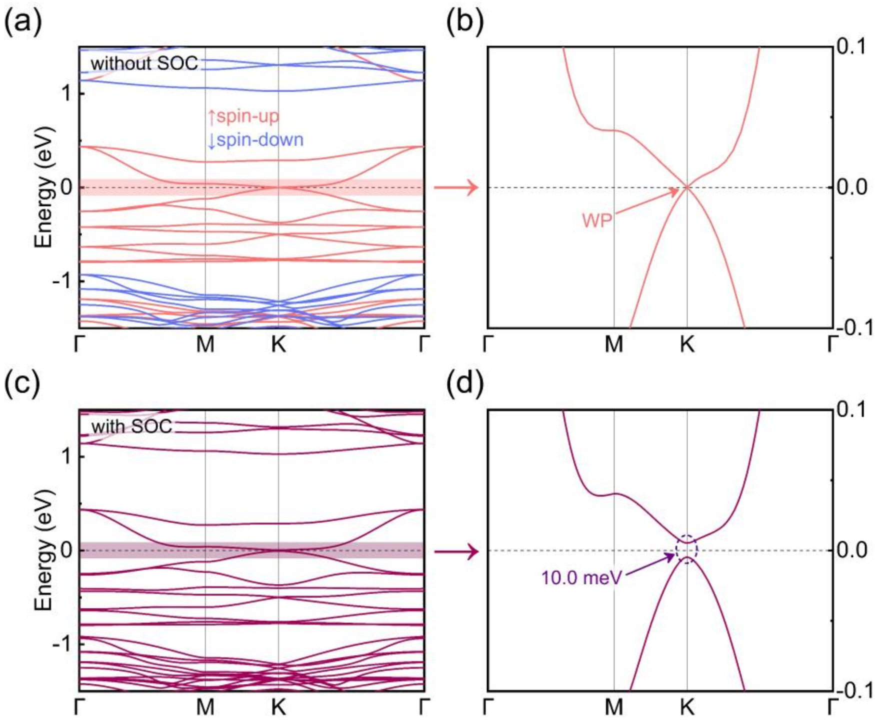

FIG. S5. Calculated electronic band structures of the $Li_{12}Zn_{10}Cr_2P_{12}$ monolayer (a) without SOC and (c) with SOC. (b) and (d) are enlarged view around the Fermi energy level.

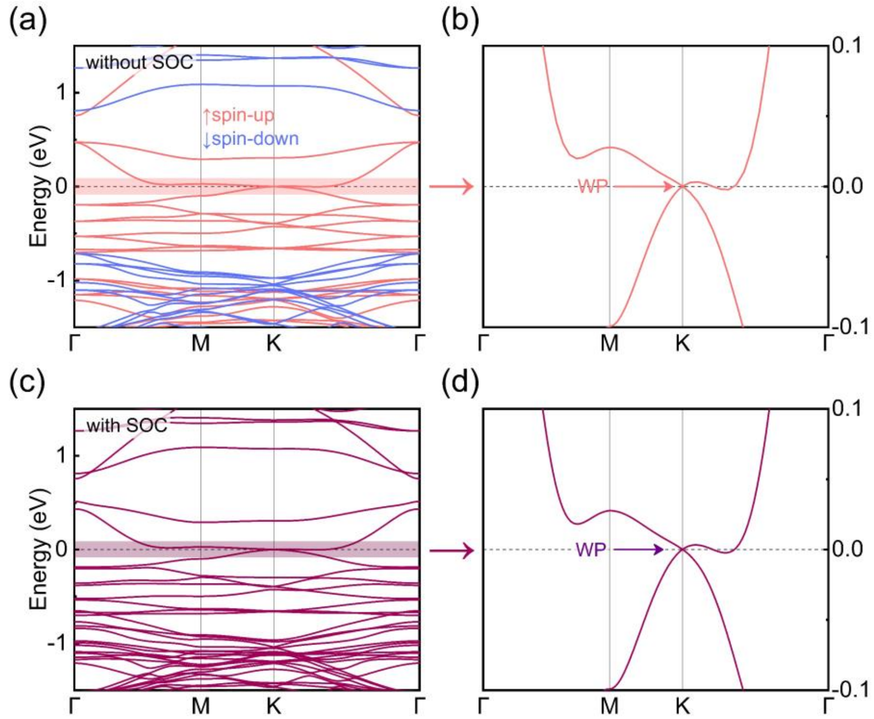

FIG. S6. Calculated electronic band structures of the $Li_{12}Zn_{10}Cr_2As_{12}$ monolayer (a) without SOC and (c) with SOC. (b) and (d) are enlarged view around the Fermi energy level.

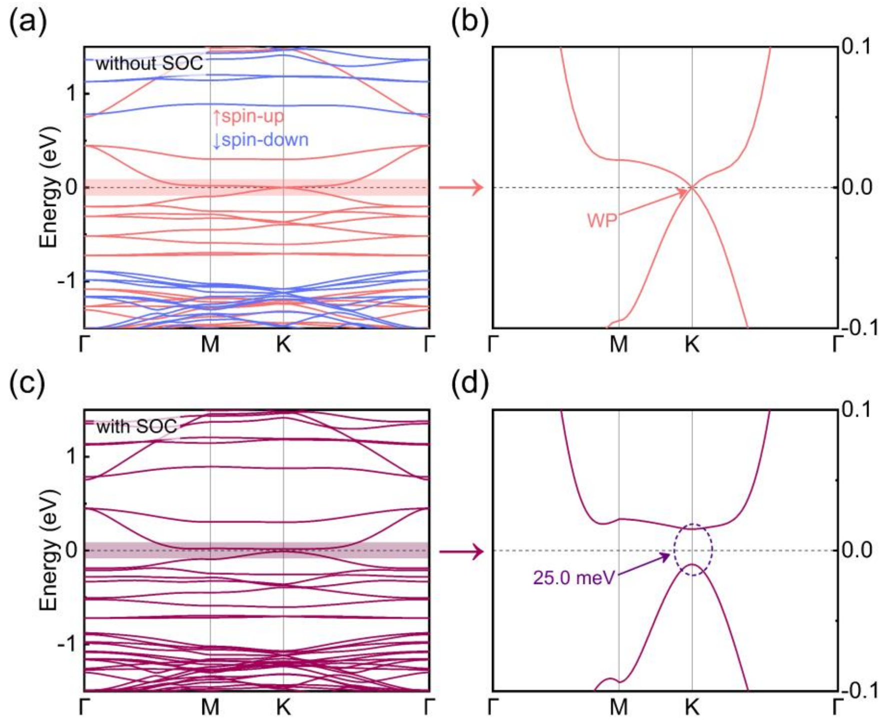

FIG. S7. Calculated electronic band structures of the $Li_{12}Cd_{10}Cr_2P_{12}$ monolayer (a) without SOC and (c) with SOC. (b) and (d) are enlarged view around the Fermi energy level.

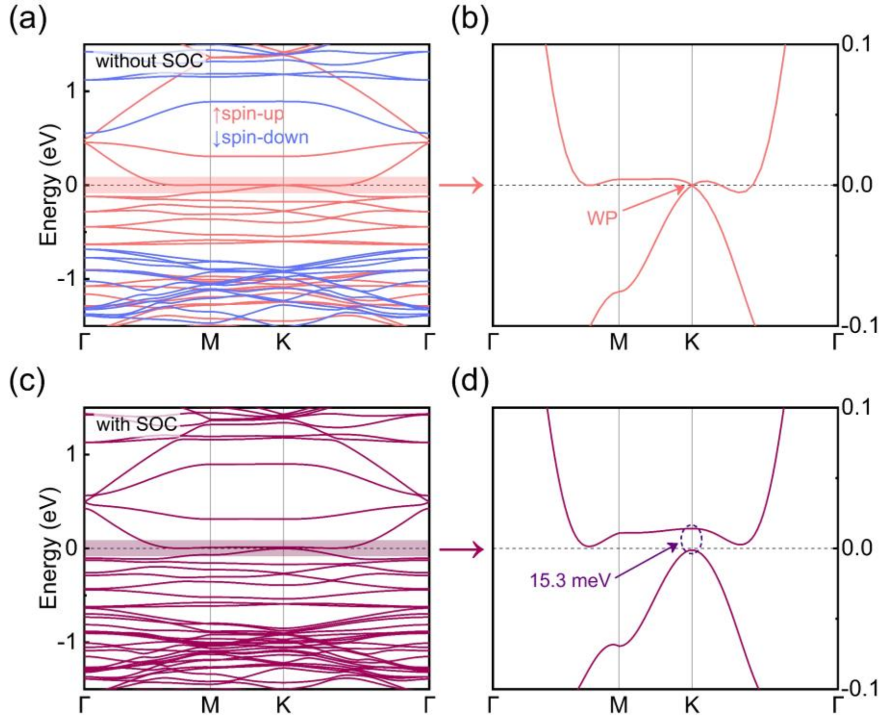

FIG. S8. Calculated electronic band structures of the $Li_{12}Cd_{10}Cr_2As_{12}$ monolayer (a) without SOC and (c) with SOC. (b) and (d) are enlarged view around the Fermi energy level.

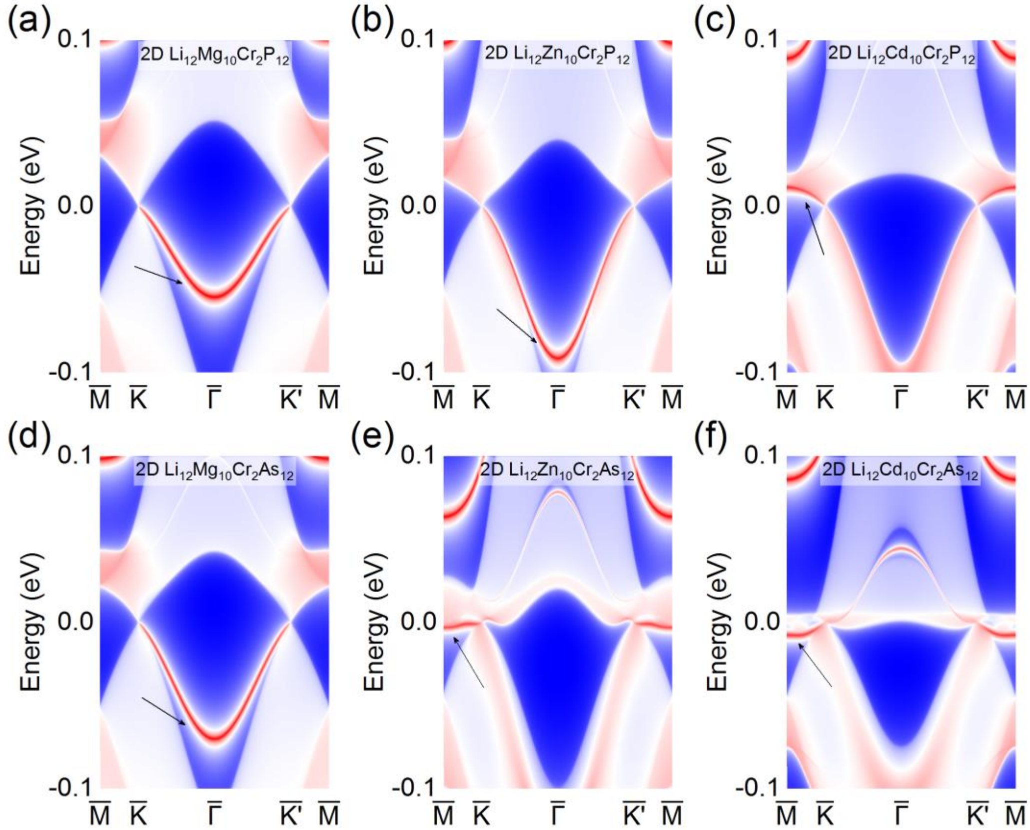

FIG. S9. Calculated The edge states along (1 0 0) surface direction without SOC of (a) $Li_{12}Mg_{10}Cr_2P_{12}$ monolayer, (b) $Li_{12}Zn_{10}Cr_2P_{12}$ monolayer, (c) $Li_{12}Cd_{10}Cr_2P_{12}$ monolayer, (d) $Li_{12}Mg_{10}Cr_2As_{12}$ monolayer, (e) $Li_{12}Zn_{10}Cr_2As_{12}$ monolayer and (f) $Li_{12}Cd_{10}Cr_2As_{12}$ monolayer, respectively.

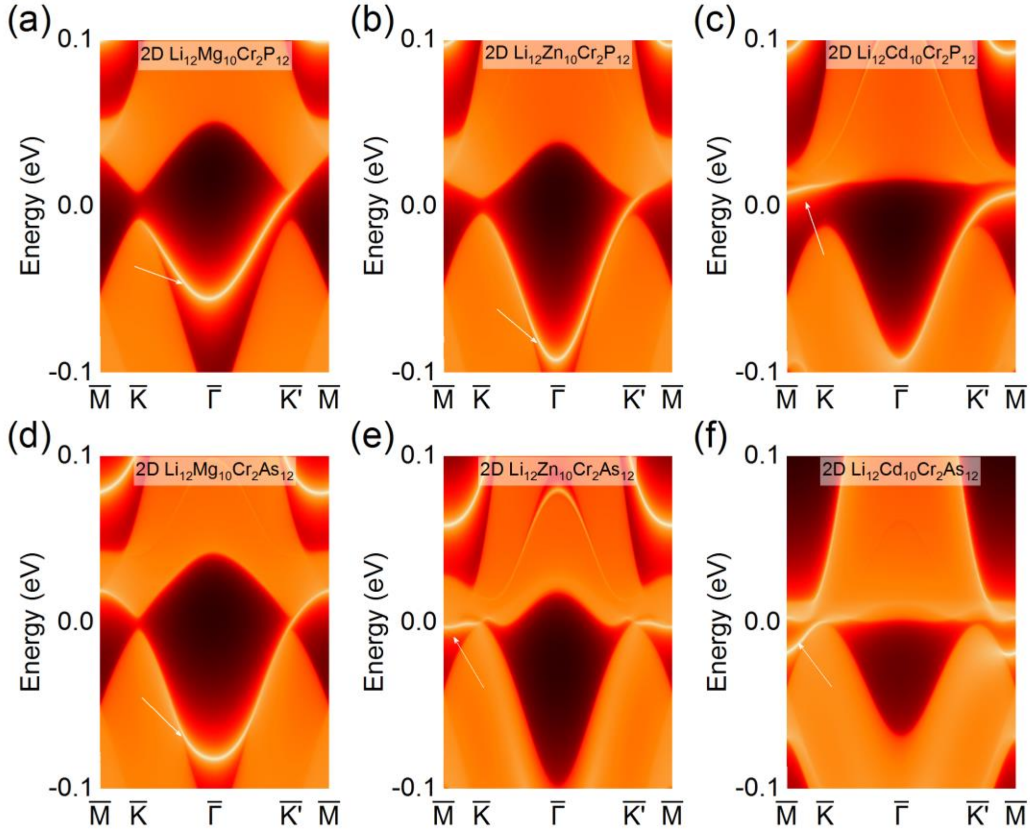

FIG. S10. Calculated The edge states along (1 0 0) surface direction with SOC of (a) $Li_{12}Mg_{10}Cr_2P_{12}$ monolayer, (b) $Li_{12}Zn_{10}Cr_2P_{12}$ monolayer, (c) $Li_{12}Cd_{10}Cr_2P_{12}$ monolayer, (d) $Li_{12}Mg_{10}Cr_2As_{12}$ monolayer, (e) $Li_{12}Zn_{10}Cr_2As_{12}$ monolayer and (f) $Li_{12}Cd_{10}Cr_2As_{12}$ monolayer, respectively.

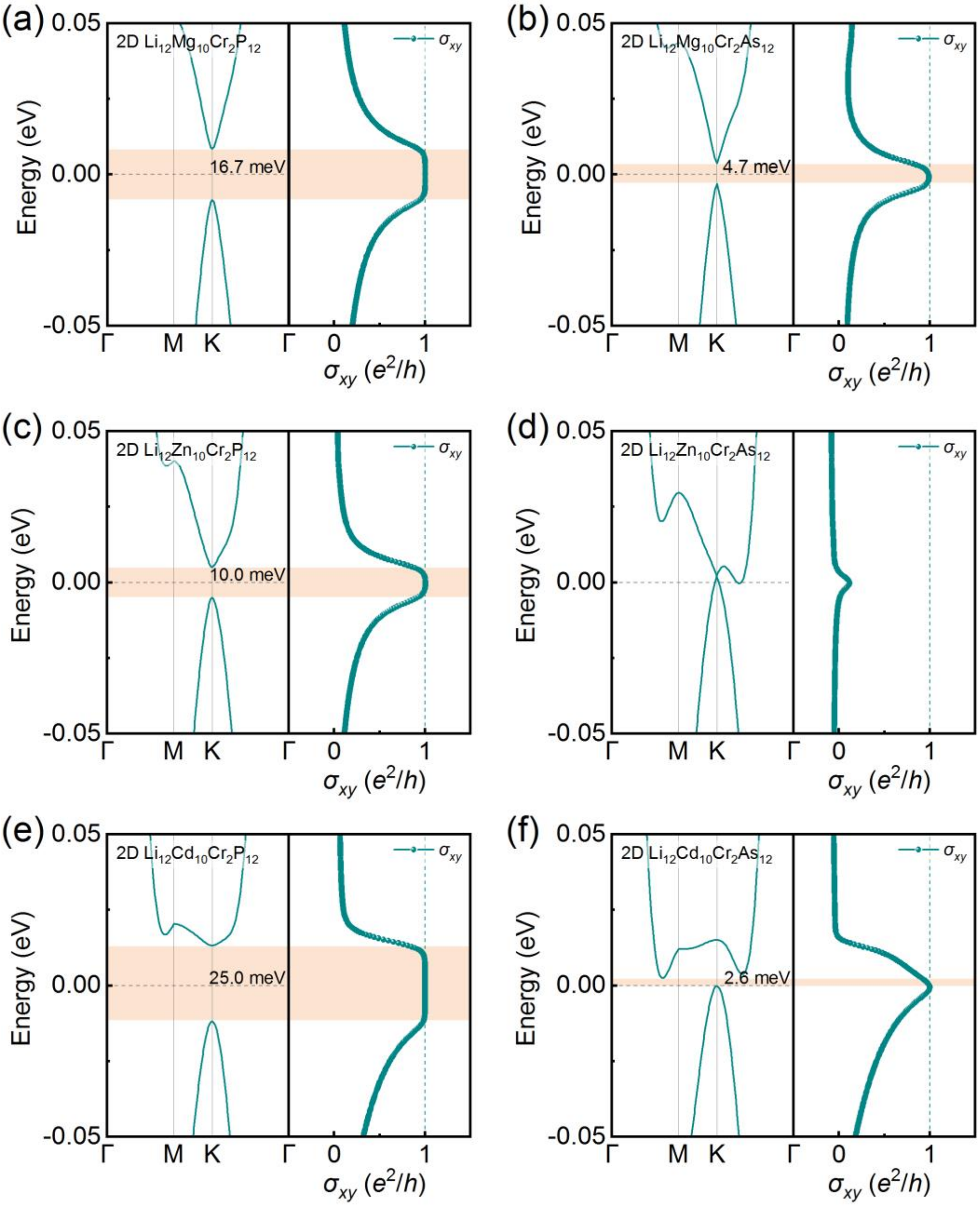

FIG. S11. Calculated band structures and anomalous Hall conductance with SOC of (a) $Li_{12}Mg_{10}Cr_2P_{12}$ monolayer, (b) $Li_{12}Mg_{10}Cr_2As_{12}$ monolayer, (c) $Li_{12}Zn_{10}Cr_2P_{12}$ monolayer, (d) $Li_{12}Zn_{10}Cr_2As_{12}$ monolayer, (e) $Li_{12}Cd_{10}Cr_2P_{12}$ monolayer and (f) $Li_{12}Cd_{10}Cr_2As_{12}$ monolayer, respectively.